TELKOMNIKA, Vol.17, No.5, October 2019, pp.2258~2267
ISSN: 1693-6930, accredited First Grade by Kemenristekdikti, Decree No: 21/E/KPT/2018
DOI: 10.12928/TELKOMNIKA.v17i5.12816

Antenna array design with rectangular ring slot for 5G technology

Nur Ilham Aliyaa Ishak[1], Norhudah Seman*[2], Tien Han Chua[3]
Wireless Communication Center, School of Electrical Engineering, Faculty of Engineering,
Universiti Teknologi Malaysia, 81310 UTM Johor Bahru, Johor, Malaysia
*Corresponding author, e-mail: aliyaa_ishak@yahoo.com[1], huda@fke.utm.my[2], thchua@fke.utm.my[3]

Abstract

A patch antenna with rectangular-shaped ring slot that fed by a coaxial probe is proposed in this article as the single element for planar patch array antenna design to meet the requirement of multiple input multiple output (MIMO) in fifth generation (5G) technology. Initially, the single antenna element is designed at three different center frequencies of 0.85, 1.9 and 2.6 GHz to cover the mobile operating frequency of 0.8, 0.85, 0.9, 1.8, 2.1 and 2.6 GHz, which considering the proposed 5G spectrum below than 6 GHz. The rectangular-shaped ring slot is introduced to the patch antenna with the partial ground plane to widen the bandwidth performance. The designed single element is then arranged to design planar arrays of 2x2. Each of elements in the planar array is fed by a coaxial probe. The designs are utilizing a high-performance substrate, Rogers 6010LM.

Keywords*: 5G technology, MIMO, patch antenna, planar antenna array, rectangular slot*

1. Introduction

Fifth generation (5G) is an advanced technology that enables the device-to-device, vehicle-to-vehicle and smart devices to communicate [1] with efficiently utilizing the existing and expanded bandwidth (BW), while managing the system requirements. This future technology is planned to be launched between 2020 and 2030 with 1000 times of system capacity, 10 times spectral and energy efficiency, 25 times average call throughput [1–3] and five times reduced end-to-end latency for higher data rates [4] and advanced speed beyond the current fourth generation (4G) of Long-Term Evolution (LTE). The new generation of 5G technology concerns the requirement of a number of antennas where the multiple input multiple output (MIMO) system with this multiple antennas are the expected elements to be integrated into the global network to fulfill the 5G requirement [2, 4–10]. Several researches on MIMO system for 5G technology has been discovered in [1, 2, 4] to predict the scenario and environment of the future mobile technology of 5G network.

Microstrip patch antenna is the most preferable antenna type for the MIMO system as it promises several advantages in terms of manufacturing cost, low profile design and excellent performance [3, 6, 7, 11-15]. Early in 2000 [16], 1x4 microstrip patch array antenna is proposed to handle the MIMO system in increasing the wireless network capacity. The U-shaped slot is introduced to provide the dual-band behavior. This array antenna also offers a simple yet compatible for almost every wireless application, which parallels to the goals of 5G technology visualization of “Internet of Things” (IoT) that integrated, reachable and accessible simultaneously. The conventional microstrip patch array antennas with 1x2 and 1x4 configurations have been designed in [9, 10] for specific absorption rate investigation using the high-performance substrate of Rogers RT6010LM. However, the research is limited to linear patch antenna array and the overall dimension of the array seems large. While, the 1x4 linear antenna array with Archimedean spiral slot for multiband frequencies is proposed in [17]. Three Wilkinson power divider are implemented to form the antenna array. Nevertheless, the work is limited to linear antenna array as well. Meanwhile in [10], the 16 antenna-element of 4x4 configuration is designed as a basis to develop the arrays with 64,128 and 256 antenna-element that fed by coaxial probe. Yet, the single antenna has a complex design. Another research of microstrip patch antenna with U-shaped is designed in [18] with configurations of 1x2, and 2x2 for MIMO applications. The U-shaped slot is designed to improve the bandwidth of

Received October 15, 2018; Revised March 28, 2019; Accepted April 27, 2019

the conventional patch and increase the length of the equivalent surface current path. While recent researches on microstrip patch antenna for MIMO system in [11, 13] are applicable for higher frequency up to more than 60 GHz. The 1x6 U-shaped slotted elements with fused silica material and dual grounded coplanar waveguide (GCPW) feeding is designed purposely for mm-wave MIMO application for a higher frequency band of 57-63 GHz [19]. The six-element array is chosen to provide sufficient gain and suit for the indoor MIMO channel measurements, which integrated with the RF chipset. The designed U-slotted antenna is capable of beam steering up to ±40° from the broadside. While in [9], the 1x4 elements of T-shaped patches that realized by Rogers RT Duroid 5880 material is designed to achieve a targeted bandwidth of 12.4 GHz, covering from 25.1-35.1 GHz. This design also introduced the defect ground structure (DGS) approach to improve the bandwidth performance of the conventional microstrip patch antenna. The defect ground act as a resonant gap to allow the efficient coupling with the feed line by changing the effective capacitance and inductance response through the excitation and electromagnetic propagation along the substrate. However, the T-shaped radiating element with coplanar-waveguide feed limits the antenna to perform in the planar array configuration. As the MIMO system in 5G technology dealing with hundreds of antennas, this approach does not quite suit the 5G requirement.

Thus, this article proposed a new design of microstrip patch antenna with a rectangular-shaped ring slot that fed by a coaxial probe for mobile operating frequencies from 0.80 to 2.6 GHz utilizing the CST Microwave Studio 2016. The gap, g which represents the slot size and coaxial probe location are analyzed to obtain the best performance of this proposed antenna. This single element microstrip patch antenna is then applied in the design of 2x2 planar array configuration. Each element of this planar array antenna is fed individually, which can perform as a single antenna, 1x2 linear array and 2x2 planar array.

2. Antenna Design

Primarily, a microstrip patch antenna as depicted in Figure 1 and Figure 2 is designed at three center frequencies of 0.85, 1.9 and 2.6 GHz to cover the respective designated frequencies of 0.8, 0.85, 0.9, 1.8, 2.1 and 2.6 GHz. The top layer of the designed antenna consists of two radiating elements, named as Patch 1 and Patch 2 that separated by a narrow gap with a dimension of g (rectangular-shaped ring slot). This narrow gap, g is implemented purposely to separate the rectangular patch into two parts, which leads to broadening the bandwidth performance of the antenna. Whilst, the partial ground plane technique is applied in the antenna design to widen the bandwidth performance [20], where two parallel rectangular ground planes are placed at the bottom of the antenna to mount the coaxial feed. The coaxial feed is positioned close to the edge and in between two rectangular ground planes.

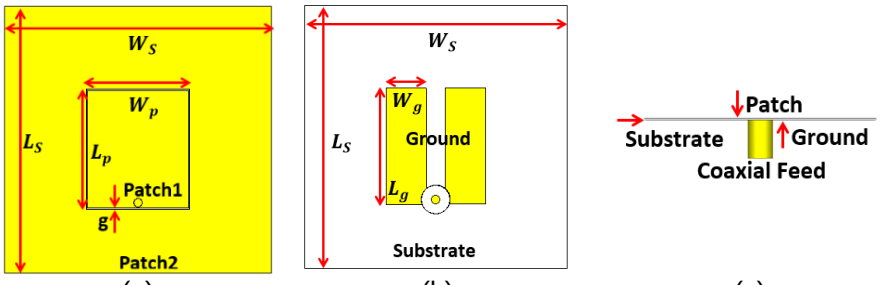

Figure 1. The layout of rectangular patch antenna design (a) top, (b) bottom and (c) side view

The coaxial feed of this antenna is designed for 50Ω matching to maximizing the power transmission with a typical dimension of 0.64 mm for inner radius of the pin and 2.15 mm for outer radius of cover. Teflon material is selected for the dielectric coating to isolate the pin and the cover. The coaxial feed is positioned and tested for three different locations starting from edge of the patch at (0, 0.97), to (0, 1.07) and (0, 1.17) for 0.85 GHz, (0, 1.15) to (0.1.25) and

(0, 1.35) for 1.9 GHz and (0, 0.79), to (0, 0.89) and (0, 0.99) for 2.6 GHz to obtain the optimal 50Ω matching as illustrated in Figure 3 and summarized in Table 1. P1 is the best coaxial feed locations, which are 0.97 mm, 1.15 mm and 0.79 mm above the edge of the patch for the respective center frequencies of 0.85 GHz, 1.9 GHz and 2.6 GHz according to the reflection coefficients, S_{11}. However, for the center frequency of 1.9 GHz, the best location of coaxial feed at (0, 1.15) demonstrates the worst S_{11} of -4.20 dB. After all, this antenna performs a dual-band operation, which at designated frequencies of 1.8 GHz and 2.1 GHz that allows for the coaxial feed location P1 with S_{11} of -4.20 dB to be accepted. Patch 1 and Patch 2 allow the maximum free electron to move back and forth between the patches to the source of power excitement at the optimum 50Ω of matching state to operate at 1.8 GHz and 2.1 GHz.

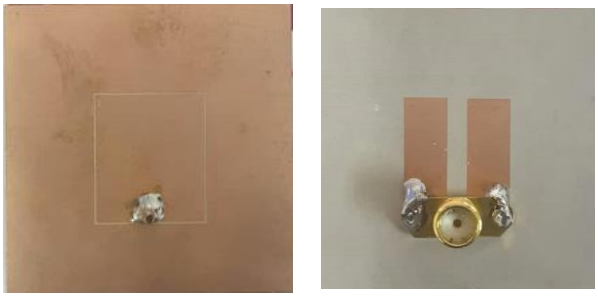

(a) (b)

Figure 2. The fabricated rectangular patch antenna (a) top and (b) bottom view

Table 1. The Designed Antenna S_{11} of Three Coaxial Feed Locations for Different Center Frequencies, f_c

f_c = 0.85 GHz		f_c = 1.9 GHz		f_c = 2.6 GHz	
Location (x,y)	S_{11}	Location (x,y)	S_{11}	Location (x,y)	S_{11}
P3 (0,1.17)	-0.16	P3 (0,1.35)	-3.72	P3 (0,0.99)	-7.69
P2 (0,1.07)	-14.31	P2 (0,1.25)	-3.77	P2 (0,0.89)	-11.04
P1 (0,0.97)	-14.96	P1 (0,1.15)	-4.20	P1 (0,0.79)	-21.44

The initial length, L_p and width, W_p dimension of Patch 1 are designed based on the respective (1) and (2) [21]:

$$L_p = \left(c/2f_r\sqrt{\varepsilon_{eff}}\right) - 2\Delta L \quad (1)$$

$$W_p = (c/2f_r)\sqrt{2/(\varepsilon_r + 1)} \quad (2)$$

where $c, f_r, \varepsilon_{eff}, \varepsilon_r$ and ΔL are the speed of light, designated frequency, the effective dielectric constant, the dielectric constant of the substrate and the normalized extension in the length due to the fringing effect, accordingly. The effective dielectric constant, ε_{eff} and the normalized extension in the length, ΔL can be determined through the respective expression in (3) and (4) [21]:

$$\varepsilon_{eff} = ((\varepsilon_r + 1)/2) + ((\varepsilon_r - 1)/2)\left[1 + 12\left(h/W_p\right)\right]^{1/2} \quad (3)$$

$$\Delta L = 0.412h\frac{(\varepsilon_{eff} + 0.3)\left(\left(W_p/h\right) + 0.2\right.}{(\varepsilon_{eff} - 0.258)\left(\left(W_p/h\right) + (\right.} \quad (4)$$

where h is the thickness of the substrate. Meanwhile, Patch 2 is designed to have the width and length that similar to the substrate's width, W_s and length, L_s. The dimension of substrate length, L_s and width, W_s are computed based on the respective $2.13L_p$ and $1.9W_p$. While gap, g is designed from the coplanar approach to obtain a wider bandwidth. The analytical line impedance calculation built in the software used to determine the exact gap width. This gap, g serves a surface current between Patch 1 and Patch 2 that can be shown by the surface current distribution analysis that will be explained in the following section. In addition, the width, W_g of two parallel rectangular ground planes is designed to be equal to $0.38\,L_p$, while its length, L_g is similar to L_p. Initially, only a single rectangular ground is designed, which have a similar size to Patch 1's dimension. Then, a square slot with length of L_g is placed in the middle of the rectangular plane that cut the feeding location. Thus, the ground plane is not short-circuited the coaxial pin. The width of the square slot is optimized to have the best performance of the antenna and the coaxial feed is able to be mounted at the optimal location, which explained next. Although the coaxial feed has a narrow bandwidth property [21], this feeding technique offers a practical design for MIMO system specifically for the planar array.

Subsequently, this single antenna is then used to form an antenna planar array in the configuration of 2x2 with several significant optimizations to stimulate the MIMO application of 5G technology as shown in Figure 4. The width, W_s and length, L_s for each element of the planar array designed, is accustomed at each designated center frequency to obtain the optimal performance. The slightly extended dimension of $0.32W_p$ and $0.15L_p$ is applied to sustain the overall performance of the planar antenna. The separation distance of half wavelength ($\lambda/2$) is selected as it offers the optimal mutual coupling between each of the antenna element. These multiple antennae can be operated as a single, 1x2 array antenna and 2x2 array antenna as the individual feed is designed for each antenna element.

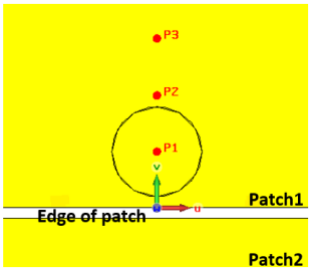

Figure 3. Three tested coaxial feed locations for the optimal 50Ω matching

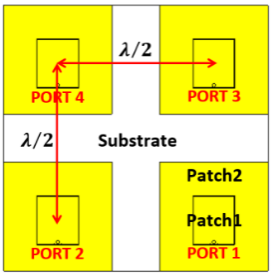

Figure 4. Planar array antenna of 2x2 configuration

The high-performance substrate, Rogers RT6010LM with 0.254 mm thickness, 10.7 of dielectric constant and 0.0023 of loss tangent is chosen for the design to attain a small size of an array antenna with good performance [22]. Furthermore, this high-performance substrate is significantly affecting the resonance frequency, bandwidth efficiency due to good thermal mechanical stability [23, 24], and the impedance matching. Furthermore, this substrate with high dielectric constant promises a high electrically polarized characteristic that enables the material to store more charges, which will end up with small electronic circuits. Dielectric constant, ε_r can be derived as the ratio of the permittivity of the dielectric to that of free space as expressed in (5) [25]:

$$\varepsilon_r = 1 + \chi_e = \varepsilon/\varepsilon_0 \quad (5)$$

where χ_e, ε and ε_0 are an electric susceptibility of the material, material permittivity and free space permittivity ($10^{-9}/36\pi$ F/m), accordingly. This electric susceptibility is a measure of how sensitive the dielectric material in response to an applied electric field. The greater the electric susceptibility, the greater the ability of the dielectric material to polarize in reaction to the field and store energy. Thus, the high-performance substrate in this research contributes to the compact design of the patch antenna with good performance for mobile operating frequencies.

3. Current Distribution Analysis of Rectangular Patch Antenna

Antenna is a resonant element, which assuredly dependent to the frequency selection, thus the dimension of the patch antenna is designed accordingly to the formulation given as in (1) to (4). Copper standard annealed material with 0.018 mm thickness is chosen for antenna patch as copper is a high conductivity material with a relative permeability of almost 1. These two characteristics clearly demonstrates that copper is a good material that allows the maximum number of the free electrons to move for conduction current. Microscopically, metals have an abundance of free electron due to the applied electric field. These free electrons will collide to each other and produce the conduction current density given in the point form of Ohm's Law in expression (6) [25]:

$$J = \sigma E \tag{6}$$

where J, σ and E are conduction current density, the conductivity of the conductor and the applied electric field, respectively. The antenna works when the external electric field is applied, which excited from the coaxial feed. The positive free charges pushed along the same direction as the applied field, while the negative charges move in the opposite direction as shown in Figure 5. Thus, this charge migration induced a surface current from Patch 1 that coupled to Patch 2 through rectangular-shaped ring slot with the size of the gap, g as shown in Figure 6. Referring to Figure 6, the field strength, which is red in color is more concentrated on the feed location of the antenna and distributed to the left and right of the Patch 1 and Patch 2 of the designed antenna.

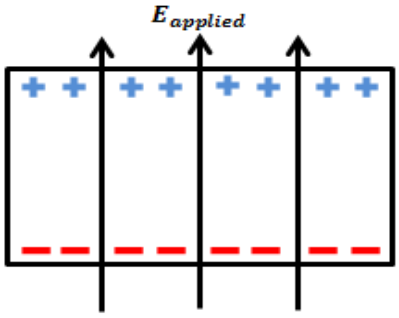

Figure 5. A conductor under the influenced of an applied field

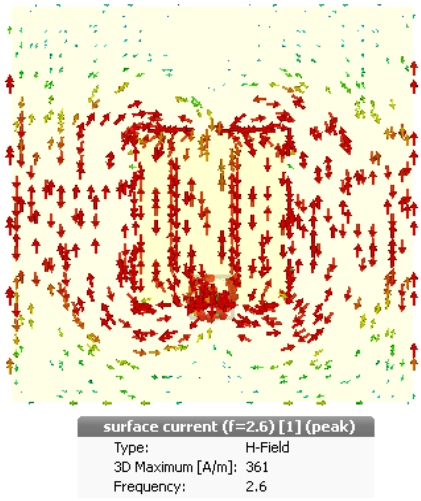

Figure 6. Surface current distribution from Patch 1 to Patch 2 of the designed antenna

Hence, the current density is closely related to the size of the gap, g. Gap, g in a form of a rectangular-shaped ring slot seems suitable for array antenna with high dielectric constant substrate fed by the coaxial for the MIMO system. This gap implementation in the microstrip patch antenna design improves the surface current density, *J*. The width of the gap, g is varied from 0.15 mm (the maximum allowable width for the fabrication) to 0.50 mm to attain the optimal surface current density of the antenna. Table 2 tabulates the surface current density of the antenna while varying the dimension of the gap, g at center frequencies of 0.85 GHz, 1.9 GHz, and 2.6 GHz. The least gap dimension of 0.15 mm performs the highest surface current density compared to the others. This is interrelated to the surface charge distribution from Patch 1 coupled to Patch 2 through the gap, g, which as the dimension of gap getting bigger, the surface charge distribution is weakened due to the smaller amount of free electron migration from Patch 1 to Patch 2. Thus, resulting to the low surface current density. Its illustration of the highest surface current distribution at 2.6 GHz for gap dimension of 0.15 mm is shown in Figure 7.

Table 2. Surface Current Density While Varying the Gap, *G* Dimension

Gap, g (mm)	Surface Current Density, *J* (A/m)		
	f_c = 0.85 GHz	f_c = 1.9 GHz	f_c = 2.6 GHz
0.15	52.10	70.78	361.0
0.20	48.80	70.78	273.6
0.25	48.80	70.78	236.9
0.30	42.89	37.25	195.5
0.35	42.89	37.25	172.0

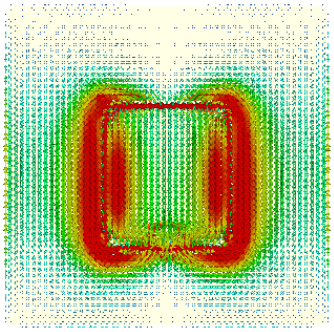

Figure 7. Surface current distribution at 2.6 GHz

4. Results and Analysis

Simulated and measured results of patch antennas are summarized in the following subsections in terms of reflection coefficient (S_{11}), gain and directivity, isolation and radiation pattern.

4.1. Reflection Coefficient (S_{11}) Performance

Reflection coefficient, S_{11} performance represents how much power is reflected from the antenna. The analysis based on the coaxial feed positioning as illustrated in Figure 3 to achieve the best S_{11} performance. The best position of coaxial feed determined the overall S_{11} performance of the antenna as it defines the maximum power transmitted. The reflection coefficients, S_{11} of the designed single rectangular patch antennas shown in Figure 1 with optimized dimension and position of coaxial feed are plotted as depicted in Figure 8 and tabulated in Table 3. The single antenna with center frequencies of 0.85 GHz performs 160 MHz bandwidth (0.77-0.93 GHz) with S_{11}<-10 dB, while 1.9 GHz performs 400 MHz (1.77-2.17 GHz) and 2.6 GHz performs the least bandwidth of 50 MHz (2.57-2.62 GHz). The single antenna with the center frequency of 1.9 GHz has the largest bandwidth with very small reflected power that less 1.7%. While, the single antenna with 0.85 GHz and 2.6 GHz center frequency have slightly higher reflected power that less than 4.0% and 6.7%, respectively. Here, to validate the concept of gap implementation in the design, single 2.6 GHz antenna as shown in Figure 2 is fabricated. The measured S_{11} that less than –10 dB demonstrates 40 MHz bandwidth (2.59-2.63 GHz), which 10 MHz narrower compared to the simulation. At 2.6 GHz, both S_{11} performances are comparable, which validate the use of narrow gap that provides the higher surface current distribution and better bandwidth performance compared to the conventional microstrip rectangular patch antenna. Afterword, the performances of the designed array antenna concerning configurations of 1x2 and 2x2 are evaluated and summarized in Table 3. From the results obtained, the 1x2 and 2x2 array with the 1.9 GHz center frequency depict the largest bandwidth of 370 MHz and 430 MHz, respectively compared to arrays with 0.85 and 2.6 GHz center frequencies. Concerning each designated mobile operating frequency, arrays' S_{11} are less than -10.12 dB. Where, this worst S_{11} performance is shown by 1x2 array at 1.8 GHz, which indicates that the antenna has the maximum reflected power of 12.9%.

4.2. Gain and Directivity Performance

Meanwhile, gain and directivity performance are another useful information for describing the antenna performance. Gain is controlling antenna efficiency in terms of radiation intensity, while directivity only describes the directional properties of the antenna in terms of the pattern. The gain and directivity performances for each designated frequency of single antennas and arrays are depicted in Table 3. The 2x2 array antenna configurations for all designated frequencies perform the highest gain and directivity compared to the single antenna and 1x2 linear array antenna. This is due to the summation of gain from the individual antennas, which is closely related to the antenna's radiation intensity. This indicates that the proposed linear and planar array antenna is superior to the single antenna in term of gain and directivity

performance as shown graphically in Figure 9. As the number of antennae increasing, the larger size of antenna is obtained, thus, a larger power is transmitted in the direction of peak radiation from an isotropic source. Specifically, the 2x2 array at 2.1 GHz performs the highest the gain and directivity amongst the designated frequencies, which are 8.35 dB and 8.36 dBi, respectively. Thus, the proposed array antennas appear to be capable to handle the MIMO structure with improved performance in terms of gain and directivity compared to the single antenna. Hence, these array antennas seem to have a feature that supports the diversity scheme of MIMO system for improving the reliability of information signal.

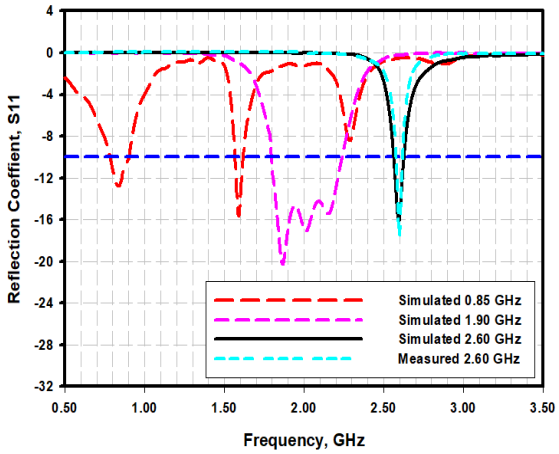

Figure 8. Single antennas S_{11} performance

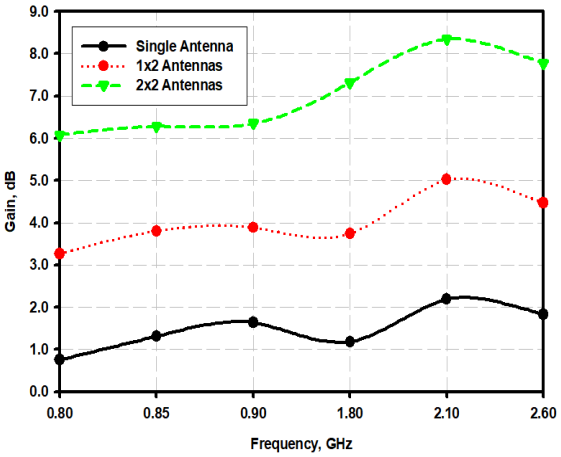

Figure 9. Gain performance for single antenna and arrays

Table 3. Single, 1x2 and 2x2 Antenna Array Performances of S_{11}, Gain, Directivity, 3 dB Beamwidth and Bandwidth

Type	Frequency (GHz)	S_{11} (dB)	Gain (dB)	Directivity (dBi)	3 dB Beamwidth (Degree)	Bandwidth (MHz)
Single	0.80	-14.32	0.756	0.992	260.7	
	0.85	-24.17	1.31	1.47	252.7	160
	0.90	-13.24	1.64	1.73	242.6	
	1.80	-14.26	1.18	1.04	263.8	
	2.10	-17.71	2.19	2.18	87.1	400
	2.60	S_{11s}=-12.16 S_{11m}=-17.51	1.83	2.17	88.0	BW_s=50 BW_m=30
1x2 Array	0.80	-20.13	3.26	3.22	63.4	
	0.85	-12.82	3.80	3.91	58.8	210
	0.90	-10.49	3.89	4.08	56.0	
	1.80	-10.12	3.74	3.54	58.9	
	2.10	-14.02	5.02	5.00	50.2	370
	2.60	-18.26	4.47	4.71	53.9	50
2x2 Array	0.80	-10.84	6.08	6.03	60.0	
	0.85	-13.08	6.28	6.42	56.2	110
	0.90	-10.21	6.35	6.70	53.7	
	1.80	-11.07	7.32	7.04	57.0	
	2.10	-14.28	8.35	8.36	49.5	430
	2.60	-16.16	7.78	8.19	53.8	50

4.3. Isolation Performance

The isolation or mutual coupling between two adjacent or more antennas, whether one and/or both are transmitting or receiving, is another function to measure the antenna performance. The undesirable characteristic that caused by the energy from the radiated antenna is absorbed by the nearest antenna creates a limitation for an array antenna that leads to degradation of the antenna efficiency and altered the antenna's radiation pattern. Typically, isolation should be lower than -15 dB to obtain the maximum radiated power from the array

antenna. Hence, the optimal inter-element spacing of $\lambda/2$ is precisely chosen to minimal the mutual coupling effect. The multiple antennas for the proposed 2x2 planar array show a good performance in term of isolation performance, which listed in Table 4. The mutual coupling performances for arrays at 0.80, 0.85, 0.90, 1.8 and 2.1 GHz are given as less than -32.40 dB, -25.71 dB, -30.74 dB, -17.67 dB and -24.48 dB, respectively. Whilst, it can be observed that the isolation between the adjacent elements of the array at 2.6 GHz are worst but still significantly lower, that less than -15.96 dB as illustrated in Figure 10 and noted from Table 4. From the simulation results obtained, the proposed array antennas have a good isolation among the elements that will support a good performance of MIMO system.

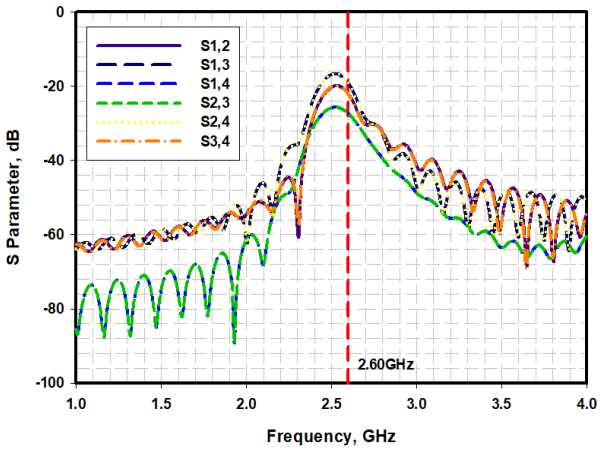

Figure 10. Isolation of 2.6 GHz array

Table 4. Isolation Performances of the 2x2 Planar Arrays

Frequency (GHz)	S_{12} (dB)	S_{13} (dB)	S_{14} (dB)	S_{23} (dB)	S_{24} (dB)	S_{34} (dB)
0.80	-32.40	-39.69	-39.65	-116.66	-39.67	-39.60
0.85	-25.71	-41.34	-41.35	-119.00	-41.30	-41.31
0.90	-30.74	-38.69	-38.69	-121.71	-38.65	-38.66
1.80	-17.67	-24.28	-28.91	-28.92	-24.26	-17.80
2.10	-24.65	-30.48	-27.28	-27.28	-30.48	-24.48
2.60	-16.12	-17.08	-22.86	-22.86	-17.08	-15.96

4.4. Radiation Pattern

Radiation pattern presents the distribution of radiated energy in the far field region, is the key performance of the antenna, where it provides information of radiation intensity, field strength, directivity, and phase. Typically, the single antenna element has relatively wide radiation pattern and low directivity, while the multiple antennas in an array configuration is an alternative to achieve high directivity with a narrow beam as can be noted from the plotted radiation patterns in Figure 11. These simulated radiation patterns at different frequencies are captured at E-field (φ=0). As the patterns for 0.8, 0.85 and 0.9 GHz are similar, only 0.85 GHz radiation pattern is shown in Figure 11. Based on the radiation patterns obtained, the single antennas for whole designated frequencies perform almost an omni-directional pattern. While, the 1x2 and 2x2 array demonstrate an almost eight-shape pattern with the main beams at 0° and 180°, which quite similar to a dipole antenna. Referring to Table 3, the 3 dB beamwidth of single antennas for all designated frequencies is broader compared to the 3 dB beamwidth of 1x2 and 2x2 array antennas. This shows that the increment of antenna adds up the maximum radiations in a particular direction.

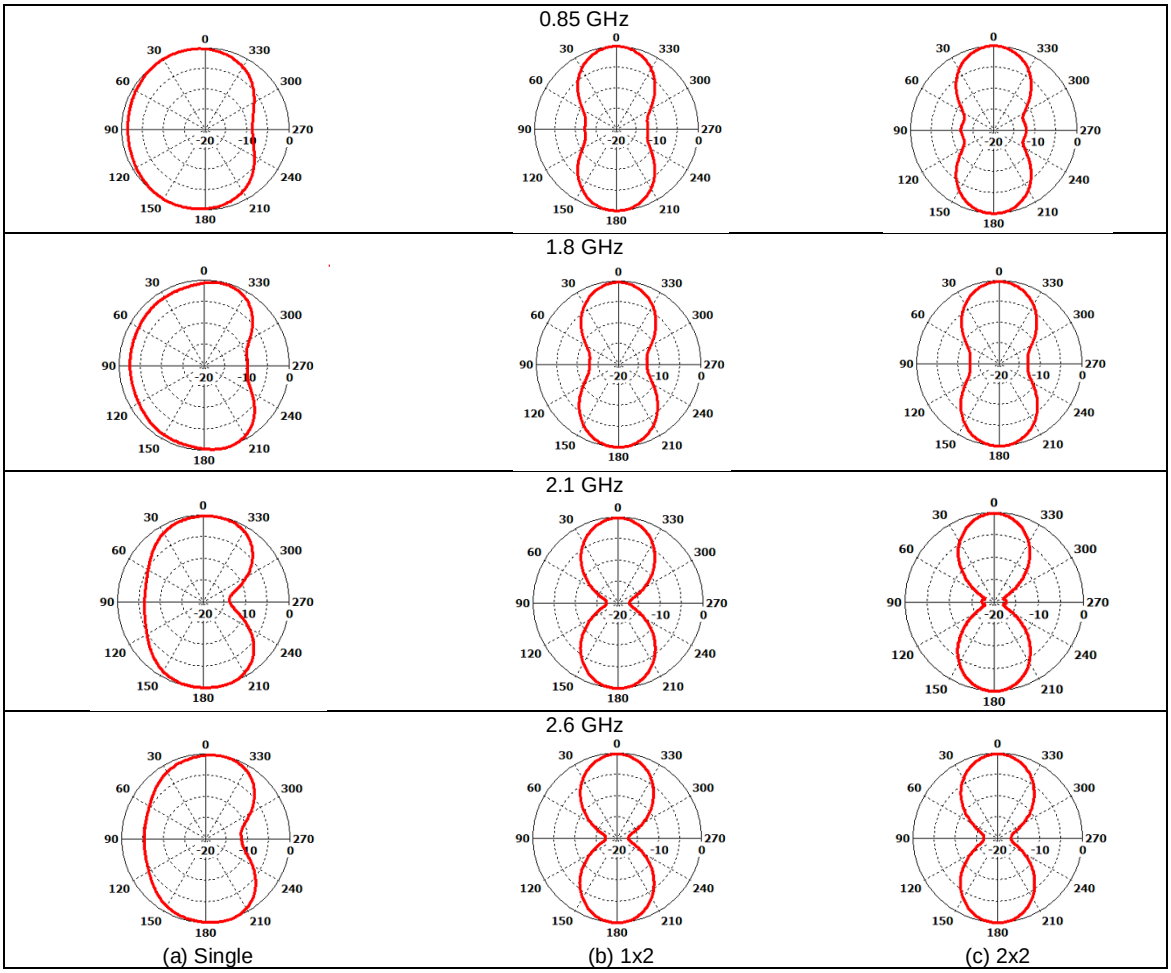

Figure 11. Radiation patterns for normalized gain at 0.85, 1.8, 2.1 and 2.6 GHz for (a) single antenna, (b) 1x2 linear array and (c) 2x2 planar array

5. Conclusion

The proposed patch antenna with rectangular-shaped ring slot and the partial ground plane has been used in the design of 2x2 planar array. The coaxial probe is utilized to feed each of elements that allows the array to perform as a single antenna, 1x2 linear array and 2x2 planar array. The designs consider three different center frequencies of 0.85, 1.9, and 2.6 GHz. These center frequencies have been chosen to cover the proposed 5G spectrum under 6 GHz concerning 0.8, 0.85, 0.9, 1.8, 2.1, and 2.6 GHz. The implementation of the rectangular-shaped ring slot in the design has improved the flow of current density that lead to the broader bandwidth. Furthermore, the interelement spacing of $\lambda/2$ in the array configuration has provided a low mutual coupling effect, which less than -15.96 dB. The proposed 2x2 planar array antenna configurations for all designated frequencies have demonstrated the performance of gain and directivity as expected compared to the single antenna and 1x2 linear array, specifically at 2.1 GHz with the gain of 8.35 dB and directivity of 8.36 dBi. Hence, the proposed planar array apparently applicable for MIMO of 5G mobile technology with high gain, directivity, lower mutual coupling, as well as good isolation between the adjacent elements.

Acknowledgements

This work was supported by Ministry of Education Malaysia (MOE) and Universiti Teknologi Malaysia (UTM) through Flagship, HiCoE, PRGS and FRGS Grant with the respective vote number of 03G41, 4J212 and 4J216, 4L684 and 5F048.

References

[1] J Sheetal. *Architecture of 5G Technology in Mobile Communication.* in Proceedings of 18th IRF International Conference. 2015. January: 43–45.

[2] X Pang, W Hong, T Yang, L Li. Design and Implementation of an Active Multibeam Antenna System with 64 RF Channels and 256 Antenna Elements for Massive MIMO Application in 5G Wireless Communications. *China Communications.* 2014; 11(11): 16–23.

[3] CX Wang *et al.* Cellular Architecture and Key Technologies for 5G Wireless Communication Networks. *IEEE Communications Magazine*. 2014; 52(2): 122–130.

[4] A Osseiran *et al.* Scenarios for 5G Mobile and Wireless Communications: The Vision of the METIS project. *IEEE Communications Magazine.* 2014; 52(5): 26–35.

[5] JG Andrews *et al.* What will 5G be?. *IEEE Journal on Selected Areas in Communications*. 2014; 32(6): 1065–1082.

[6] H Magri, N Abghour, M Ouzzif. Key Concepts of 5th Generation Mobile Technology. *International Journal of Electrical, Computer, Energetic, Electronic and Communication Engineering*. 2015; 9(4): 448–451.

[7] K Zhao, Z Ying, S Member, S He. EMF Exposure Study Concerning mmWave Phased Array in Mobile Devices for 5G Communication. *IEEE Antennas and Wireless Propagation Letters*. 2016; 15: 1132–1135.

[8] D Colombi, B Thors, C Törnevik. Implications of EMF Exposure Limits on Output Power Levels for 5G Devices Above 6 GHz. *IEEE Antennas and Wireless Propagation Letters*. 2015; 14: 1247–1249.

[9] SF Jilani, A Alomainy. *Millimetre-wave T-shaped antenna with defected ground structures for 5G wireless networks*. 2016 Loughborough Antennas and Propagation Conference, LAPC 2016. 2017; Lapc 2016: 8–13.

[10] H Yuan, C Wang, Y Li, N Liu, G Cui. *The Design of Array Antennas Used for Massive MIMO System in the Fifth Generation Mobile Communicatio*n. in 2016 11th International Symposium on Antennas, Propagation and EM Theory (ISAPE). 2016: 75–78.

[11] RJ Mailloux, JF McIlvenna, NP Kernweis. Microstrip Array Technology. *IEEE Transactions on Antennas and Propagation*. 1981; 29(1): 25–37.

[12] J James, P Hall. Handbook of Microstrip Antennas. Stevenage, United Kingdom: Institution of Engineering and Technology (IET). 1989; 2(2).

[13] IJ Bahl, P Bhartia. *Design Considerations in Microstrip Antenna Fabrication.* in 10th European Microwave Conference, 1980. 1980: 122–126.

[14] MRIMRI Faruque, MIMI Hossain, MTMT Islam, MIMI Hossain. Low specific absorption rate microstrip patch antenna for cellular phone applications. *IET Microwaves, Antennas & Propagation.* 2015; 9(14): 1540–1546.

[15] TAJ Mary, SJ Priyadarshini, CS Ravichandran, D Sugumar. *Investigation of SAR on Human Head Modelling using Patch Antenna in Mobile Communication for Dual Band Frequency*. International Conference on Emerging Trends in Robotics and Communication Technologies, INTERACT-2010. 2010: 121–124.

[16] N Crispim, R Peneda, C Peixeiro. *Small Dual-Band Microstrip Patch Antenna Array for MIMO System Applications.* in IEEE Antennas and Propagation Society Symposium. 2004; 1: 237–240.

[17] W Zhou, T Arslan. *A Bidirectional Planar Monopole Antenna Array for WiFi/Bluetooth and LTE Mobile Applications.* in 2013 Loughborough Antennas & Propagation Conference (LAPC), 2013. 2013; 1(November): 186–189.

[18] W Swelam, M Ali Soliman, A Gomaa, T Taha. *Compact Dual-Band Microstrip Patch Array Antenna for MIMO 4G Communication Systems.* in IEEE Antennas and Propagation Society Symposium. 2010; 1(1): 94–100.

[19] M Salarpour, F Farzaneh, RB Staszewski. *Design Procedure of a U-Slot Patch Antenna Array for 60 GHz MIMO Application.* in 2018 14th International Conference on Advanced Trends in Radioelecrtronics, Telecommunications and Computer Engineering (TCSET). 2018: 612–615.

[20] J Kumar, SS Shirgan. *Compact Partial Ground Plane 1x2 Patch Antennas.* Proceedings 2014 6th International Conference on Computational Intelligence and Communication Networks, CICN 2014. 2014: 33–37.

[21] CE Balanis. Antenna Theory: Analysis and Design. 3rd Edition. Hoboken, New Jersey: John Wiley & Sons, Inc. 2005.

[22] JY Chung, PM Nguyen. Characterisation of antenna substrate properties using surrogate-based optimisation. *IET Microwaves, Antennas & Propagation*. 2015; 9(9): 867–871.

[23] MHM Salleh, N Seman, R Dewan. The Investigation of Substrate's Dielectric Properties for Improving the Performance of Witricity Devices. *Applied Computational Electromagnetics Society Journal*. 2017; 32(1): 24–30.

[24] NN Al-areqi, N Seman, TA Rahman. Parallel-Coupled Line Bandpass Filter Design Using Different Substrates for Fifth Generation Wireless Communication Applications. 2015: 3–6.

[25] MN Sadiku. Element of Electromagnetics, Internatio. New York, United States: Oxford University Press Inc. 2014.